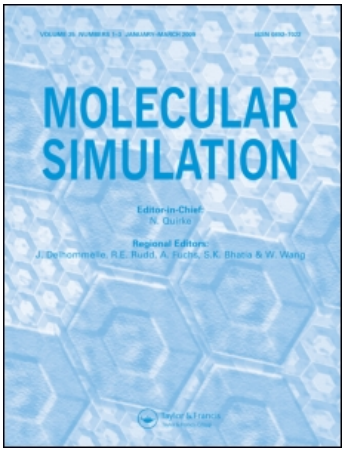

Molecular Simulation
Publication details, including instructions for authors and subscription information:
http://www.informaworld.com/smpp/title~content=t713644482

Molecular Dynamics Simulations for 1:1 Solvent Primitive Model Electrolyte Solutions

Soong-Hyuck Suh[a]; Jae-Woo Park[a]; Ki-Ryong Ha[a]; Soon-Chul Kim[b]; James M. D. Macelroy[c]
[a] Department of Chemical Engineering, Keimyung University, Taegu, South Korea [b] Department of Physics, Andong National University, Andong, South Korea [c] Department of Chemical Engineering, University College Dublin, Dublin 4, Republic of Ireland

To cite this Article Suh, Soong-Hyuck , Park, Jae-Woo , Ha, Ki-Ryong , Kim, Soon-Chul and Macelroy, James M. D.(2001) 'Molecular Dynamics Simulations for 1:1 Solvent Primitive Model Electrolyte Solutions', Molecular Simulation, 27: 5, 387 — 403
To link to this Article: DOI: 10.1080/08927020108031360
URL: http://dx.doi.org/10.1080/08927020108031360

Molecular Simulation, Vol. 27, pp. 387–403
Reprints available directly from the publisher
Photocopying permitted by license only

MOLECULAR DYNAMICS SIMULATIONS FOR 1:1 SOLVENT PRIMITIVE MODEL ELECTROLYTE SOLUTIONS

SOONG-HYUCK SUH[a,*], JAE-WOO PARK[a], KI-RYONG HA[a], SOON-CHUL KIM[b] and JAMES M.D. MACELROY[c]

[a]*Department of Chemical Engineering, Keimyung University, Taegu 704-701, South Korea;* [b]*Department of Physics, Andong National University, Andong 760-749, South Korea;* [c]*Department of Chemical Engineering, University College Dublin, Belfield, Dublin 4, Republic of Ireland*

(Received June 2001; In final form July 2001)

Molecular dynamics (MD) simulations at constant temperature have been carried out for systems of 1:1 solvent primitive model (SPM) electrolyte solutions. Equilibrium thermodynamics, mean cluster size, self-diffusion coefficients, and collision frequencies were computed to examine the electrostatic effects on the structural and dynamical properties. Coherent ionic cluster motion was deduced from a cluster analysis and from the dependence of the velocity and force autocorrelation functions (FACFs). The resulting MD data for the collision frequencies and self-diffusivities of both ions and hard-spheres were shown to be in good agreement with the theoretical predictions.

Keywords: Molecular dynamics simulation; Solvent primitive model electrolyte solution; Ionic cluster; Self-diffusion coefficient; Extended Enskog theory

INTRODUCTION

This article, dedicated to Dr David Nicholson, is concerned with molecular dynamics (MD) studies to investigate the structural and transport properties of electrolyte solutions. Among the various theoretical and simulation studies for electrolyte solutions, one of the simplest but most commonly used model systems in the bulk and at interfaces is the so-called "primitive model electrolyte solution" [1]. Within the framework of the primitive model (PM) of electrolyte solutions,

*Corresponding author. E-mail: shsuh@kmu.ac.kr

the charged hard-sphere ions are immersed in a continuum solvent represented only as a uniform medium of fixed relative permittivity (or dielectric constant). A major drawback in this approach is the use of the solvent continuum assumption in which the solvent structural effects are totally ignored.

In many situations a more detailed representation of the solvent molecules seems necessary and the simplest possible model for the solvent, which retains particulate structure is known as the solvent primitive model (SPM). In this simple model, which is essentially an extension of the PM to multicomponent form, the solvent particles are treated as neutral hard-spheres of finite size. Although the SPM is clearly an oversimplification in its description of the solvent molecules, an important improvement over PM electrolytes has been observed particularly for systems of high electrolyte concentration where the exclusion packing effects and the short-ranged repulsive interactions are increasingly significant.

Davis and his co-workers [2–4] have successfully applied the SPM electrolytes in their studies of the thermodynamic and structural properties of electric double layers and the effects of solvent exclusion on the force between charged surfaces in electrolyte solutions. In their Monte Carlo studies [3], it was observed that the finite size of the solvent particles resulted in highly ordered layering of ions, which was not captured in the PM electrical double layer. Forciniti and Hall [5] have investigated the equilibrium structure and the thermodynamics of SPM electrolytes, ranging from restricted model electrolytes of the same size to highly asymmetric electrolytes of different sizes, using the hypernetted chain approximation. They found a rather complex but strong correlation between nonelectrostatic and electrostatic contributions to the free energy.

More recently, molecular simulations using both the canonical [6,7] and the grand canonical [8] Monte Carlo (MC) methods have been employed to evaluate the equilibrium thermodynamics and related configurational parameters for SPM electrolytes. In the canonical MC studies reported by Vlachy *et al.* [6,7], the radial distribution functions were calculated as functions of the neutral solvent concentration and the counterion valency. Evidence of the depletion interaction effect was clearly displayed in the resulting pair correlation functions for highly asymmetric SPM electrolytes, indicating that the addition of a neutral species leads to a gradual change from repulsion to attraction in the qualitative nature of the interactions between similarly charged ions. Similar observations for PM electrolyte solutions [9,10] also suggest that the attraction between like charged macroions is possible if multivalent counterions are present in the solution, in which the valency of the counterions plays an important role in shaping the net interaction between macroions.

Almost all simulations for both PM and SPM electrolyte solutions have been carried out using the MC method. This is mainly due to one principal technical

difficulty, namely the "discontinuous" nature of hard-core repulsion combined with "continuous" soft interactions which cannot be handled properly using traditional MD methods [11]. A few implementations [12–14] have been made to extend the MD method to systems of hard cores with soft potentials. A different MD algorithm [15], referred to as the collision Verlet method, was recently introduced and is based on an extension of the general potential splitting formalism. It is interesting to note that this algorithm is nearly identical to our algorithm [14] except that our momenta are defined only at mid time step and a leap-frog formulation is employed.

In the present paper, we report MD simulation results for the system of symmetric 1:1 SPM electrolytes. In the MD method, the time-dependent transport properties, which cannot be measured by the MC method, are determined by monitoring the actual molecular trajectories as a function of time. In "Model and computations" we describe the interaction model potential and simulation parameters investigated in this work. A brief description of our MD computational techniques is also included. In "Result and discussion", we present the thermodynamic and transport properties obtained from the MD simulations including the collision frequencies, the self-diffusion coefficients, and the velocity and the force autocorrelation functions (FACFs). We also discuss in this section a cluster analysis for the mean cluster size. These simulation results for the cluster and dynamic properties are of particular interest because they can provide specific details of ion cluster formation. Our MD simulation studies can also yield insights into the interplay between short-ranged repulsive and long-ranged attractive interactions.

MODEL AND COMPUTATIONS

In the SPM electrolyte system, the solution is modeled as a mixture of charged ions (solute) and uncharged hard-spheres (solvent) with particle diameter σ immersed in a dielectric continuum ε. For solute/solvent and solvent/solvent interactions, the pair potential between particles i and j is defined as

$$u_{ij}(r) = \begin{cases} \infty & \text{if} \quad r \leq \sigma_{ij} \\ 0 & \text{if} \quad r > \sigma_{ij} \end{cases} \tag{1}$$

and, for solute/solute interactions

$$u_{ij}(r) = \begin{cases} \infty & \text{if} \quad r \leq \sigma_{ij} \\ \frac{z_i z_j e^2}{\varepsilon r} & \text{if} \quad r > \sigma_{ij} \end{cases} \tag{2}$$

where z_i and z_j are the valences of the ions, e is the charge of the electron, and the additive hard-sphere contact diameter is given by $\sigma_{ij} = (\sigma_i + \sigma_j)/2$. For the simulations investigated in this work, the uniform dielectric constant ε was chosen to be 78.365 corresponding to water at a room temperature of 298.16 K. Both the positive and negative ions have the same diameter ($\sigma_+ = \sigma_-$) of 4.25 Å and the same charge valency of 1. The diameter of the hard-sphere solvent particles (σ_0) is taken in three separate case studies to be $\sigma_0 = \sigma_+$, $\sigma_0 = 2\sigma_+$, and $\sigma_0 = 5\sigma_+$. All particles including the neutral hard-spheres have the same mass of 100 a.m.u. These parameters are chosen to allow comparisons with previous computational and theoretical studies reported in the literature.

The MD computations were carried out using the minimum image (MI) boundary condition to approximate an infinite system. The long-ranged interaction in the ionic system gives an internal configurational energy that converges slowly with increasing the system size. This is particularly true for higher concentrations and for higher charged systems. For Coulombic plasma systems [16], it has been found that the MI method is sufficiently accurate if the magnitude of a dimensionless parameter,

$$\gamma = \left(\frac{2\pi N}{3V}\right)^{1/3} \frac{(|z_i| + |z_j|)^2 e^2}{\varepsilon kT} \tag{3}$$

is below 10. In our MD simulations a total number of 200 ions ($N_+ = N_- = 100$) was used, and typical values for the parameter condition in Eq. (3) were less than 1.0. By using a sufficiently large system size, the MI method generates the same accuracy as the Ewald summation method within an acceptable error limit. We observed from a few selected MD runs that a less than 1% relative difference for the configurational energy calculations was achieved in the numerical uncertainty between the MI and the Ewald methods.

The PM or SPM electrolyte system, consisting of a hard-core repulsion with a continuous attractive interaction, gives rise to methodological problems in the MD simulation. Computational approaches in the trajectory calculations are totally different for the discontinuous and the continuous MD methods. Two distinct algorithms were combined within the same MD program by returning to the hybrid method of the "step-by-step" approach described elsewhere [14].

In our MD method the first step is identical to the procedure employed with a continuous potential. The system trajectories are advanced from the current positions to the next positions only under the influence of continuous forces without imposing the hard-core constraints. The next step is then to check whether or not the pair distances are closer than a hard-sphere collision diameter, and, in this step, the particle velocities are assumed to be constant. The algebraic

equations of colliding hard-spheres are used to evaluate the collision time between all possible colliding pairs and the resulting configuration is resolved for the overlapping pairs. For computational efficiency, it is appropriate to eliminate any redundant calculations and this was done by constructing a collider table to speed up the search routine.

The equations of motion were integrated using the leap-frog version of the Verlet algorithm with a time step interval of 10^{-14} s. The velocities were scaled at each time step to maintain constant temperature in the manner described by Berendsen *et al.* [17]. In addition, the starting configurations were generated by randomly inserting particles to assist in the equilibration of the system. Configurations were initially equilibrated for 30,000–50,000 time steps and the final statistics were obtained over $1 \times 10^7 - 2 \times 10^7$ time steps depending on the total number of particles involved.

The MD algorithm implemented in this work has been tested in a number of ways. When the solute ionic charges were assigned to a value of zero, our simulation data faithfully reproduced the pure hard-sphere results. The results obtained from our MD simulations for PM and SPM electrolytes were also compared with previous MC and MD calculations. Good agreement with simulation data reported in the literature again confirmed the quality of our MD algorithm. All simulation runs were performed on the HPC320 of the parallel computing machine at KISTI, Korea. Extensive use was made of optimization and parallelization techniques. About 40 h CPU times were taken in production runs for approximately 2000 particles and 10 million time steps.

RESULTS AND DISCUSSION

The thermodynamic and transport properties of 1:1 SPM electrolyte solutions obtained from our MD simulations are presented in Table I. In this table, $\eta_0 (= \pi/6\rho_0\sigma_0^3)$ represents the packing fraction of neutral hard-spheres with particle diameter σ_0. For the SPM state conditions, three sets of simulations were performed for $\sigma_0 = \sigma_+$, $\sigma_0 = 2\sigma_+$, and $\sigma_0 = 5\sigma_+$. The PM state point is equivalent to setting $\eta_0 = 0$ in the SPM model. We also report the self-diffusion coefficients and the collision frequencies of both solute ions and solvent hard-spheres in the last four columns, respectively.

For the SPM electrolytes the excess internal energy can be written as

$$\frac{U}{N_t kT} = \frac{2\pi\rho_t}{kT} \sum_{\alpha} \sum_{\beta} X_\alpha X_\beta \int_{\sigma_{\alpha\beta}}^{\infty} u_{\alpha\beta}(r) g_{\alpha\beta}(r) r^2 \, dr \tag{4}$$

TABLE I System characteristics and MD results for 1:1 SPM electrolyte solutions (the values in parenthesis indicate uncertainties in MD simulations)

M_+, M_- (mol/l)	η_0	N_0	$-U/N_rkT(10^{-1})$	PV/N_rkT	D_+, D_- (10^{-4} cm^2/s)	D_0 (10^{-4} cm^2/s)	ω_+, ω_- (10^{11} s^{-1})	ω_0 (10^{11} s^{-1})
$\sigma_0 = \sigma_+$								
0.1	0.0		2.7073 (0.0167)	0.9442 (0.0068)	79.614		0.4304	
	0.01	413	0.8909 (0.0064)	1.0366 (0.0068)	36.916	48.933	0.9640	0.7662
	0.02	826	0.5300 (0.0041)	1.0911 (0.0064)	23.253	28.629	1.5145	1.3261
	0.03	1239	0.3823 (0.0024)	1.1417 (0.0068)	16.906	19.992	2.1156	1.9071
2.0	0.0		6.5890 (0.0261)	1.3522 (0.0772)	5.3036		7.1183	
	0.1	207	3.3261 (0.0131)	2.2959 (0.0825)	2.3418	2.5595	18.181	17.123
	0.2	413	2.2632 (0.0086)	3.8610 (0.0978)	1.1752	1.2474	37.488	36.461
	0.3	620	1.7301 (0.0066)	6.7819 (0.1226)	0.5301	0.5479	73.991	72.922
$\sigma_0 = 2\sigma_+$								
0.1	0.1	516	0.7779 (0.0065)	1.4853 (0.0514)	17.445	10.327	2.2655	4.0071
	0.2	1033	0.4697 (0.0038)	2.3805 (0.0654)	8.0253	4.5219	5.0961	9.9440
	0.3	1549	0.3335 (0.0029)	3.9551 (0.0788)	4.1647	2.3310	9.6972	20.372
	0.4	2066	0.2656 (0.0021)	6.9428 (0.0984)	2.1820	1.0051	17.736	40.060
2.0	0.1	26	5.9853 (0.0230)	2.0197 (0.1196)	3.5845	1.9108	11.171	23.561
	0.2	52	5.4956 (0.0209)	3.2396 (0.1783)	2.2591	1.1405	17.674	39.481
	0.3	77	5.1526 (0.0194)	5.4229 (0.2469)	1.3119	0.0573	28.164	66.824
$\sigma_0 = 5\sigma_+$								
0.1	0.1	33	2.3917 (0.0207)	1.1995 (0.0929)	39.894	9.9572	0.9017	3.8515
	0.2	66	2.1739 (0.0173)	1.6907 (0.1502)	22.417	6.0433	1.5906	6.7465
	0.3	99	1.9872 (0.0162)	2.6141 (0.2292)	14.245	3.5440	2.5284	11.658
	0.4	132	1.8691 (0.0127)	4.4197 (0.3376)	8.9152	1.6312	4.0164	20.709
0.2	0.1	2	6.7413 (0.0250)	1.8373 (0.1476)	3.9751	0.4345	9.4528	79.325
	0.2	4	6.9075 (0.0252)	2.6847 (0.2294)	2.7904	0.3109	13.054	114.07
	0.3	5	7.0010 (0.0254)	3.3601 (0.2901)	2.2938	0.2503	15.635	141.25
	0.4	7	7.2131 (0.0250)	5.8603 (0.4402)	1.3519	0.1297	24.414	237.96

and, the virial expression for the osmotic pressure is

$$\frac{PV}{N_t kT} = 1 + \frac{U}{3N_t kT} + \frac{2\pi\rho_t}{3}\sum_{\alpha}\sum_{\beta} X_\alpha X_\beta \sigma_{\alpha\beta}^3 g_{\alpha\beta}(\sigma_{\alpha\beta}) \tag{5}$$

where X_i is the mole fraction of component i and $g_{ij}(\sigma_{ij})$ is the contact value of the radial distribution function between component i and j at separation distance σ_{ij}.

For ionic solutions the radial distribution function between unlike pairs changes rapidly near the contact point, and, in this case, the extrapolation to the contact value may lead to large uncertainties in MC calculations. For this reason the MC results for osmotic pressure coefficients are known to be less certain than those for the configurational energy. In the MD method better statistics can be achieved in the evaluation of the virial contribution to the equation of state for the hard-core system. The hard-core component of the instantaneous pressure can be obtained from averaging over particle collisions, and the hard-sphere collision contributions to the virial term in Eq. (5) can be directly calculated during the MD simulations as

$$\frac{PV}{N_t kT} = 1 + \frac{U}{3N_t kT} + \frac{2\pi\rho_t}{3}\frac{1}{t}\sum^{\text{coll}} \frac{2m_i m_j}{m_i + m_j}(\underline{v}_{ij}\cdot\underline{r}_{ij})\Big|_{\text{coll}}. \tag{6}$$

For the 1:1 SPM electrolyte solutions investigated here, our simulation results for the internal excess energy and the osmotic pressure have been found to be in close agreement with theoretical approximations using the mean spherical approximation [18] and the hypernetted chain theory [5,6]. Of the two approximations, the hypernetted chain predictions are closer to the MD data. With the exception of the last four entries, inspection of Table I reveals a rise in the excess internal energy upon the addition of neutral hard-spheres. Note that this value is the averaged one over the total number of particles. However, the configurational energy per ion remains almost constant at a given solvent packing fraction, η_0. The values in parentheses for the thermodynamic results reflect the statistical uncertainties estimated in our MD results, i.e. the standard deviation for block averages over 100 time step segments. Larger deviations in the osmotic pressure are measured for the system at high packing conditions due to the relatively frequent hard-sphere collisions.

The velocity autocorrelation function (VACF) can provide useful insights into ion dynamics and transport. The FACF is another important time correlation function. Although not directly related to time-dependent transport coefficients, the FACF has an important place in the theory of single particle motion. The

VACF and the FACF are defined as a function of time t, respectively,

$$\text{VACF} = \frac{1}{N}\sum_{i=1}^{N}\langle \underline{v}_i(0)\cdot\underline{v}_i(t)\rangle \tag{7}$$

and

$$\text{FACF} = \frac{1}{N}\sum_{i=1}^{N}\langle \underline{F}_i(0)\cdot\underline{F}_i(t)\rangle \tag{8}$$

where the symbol $\langle\,\rangle$ denotes an average over an equilibrium ensemble.

In Figs. 1 and 2 we display the normalized VACFs and FACFs for the two different sets of concentrations, $\rho_+ = 0.1\,\text{M}$ and $\rho_+ = 2.0\,\text{M}$, at the fixed hard-sphere size, $\sigma_0 = 5\sigma_+$, respectively, to illustrate the manner in which these functions change with increasing hard-sphere concentration η_0. As shown in these figures, the VACFs of both ions and hard-spheres for $\rho_+ = 2.0\,\text{M}$ decay more rapidly than the corresponding VACFs for $\rho_+ = 0.1\,\text{M}$. The primary mechanism for the decay of the time correlation functions is the hard-sphere collision, in which colliding particles rapidly lose memory of their initial velocities through successive collisions. The VACF_+ for the ions exhibit a stronger positive velocity correlation than the VACF_0 for the neutral hard-spheres because the Coulombic interaction plays a dominant role in determining the particle trajectories of the ions in the low concentration regime. However, at high concentrations, the hard-core repulsive collisions are expected to be the principal contribution to the dynamical properties of these systems. For the high concentration of $\rho_+ = 2.0\,\text{M}$ and $\eta_0 = 0.4$ (shown as the chain-dotted curve in Fig. 2b) the negative region of the VACF_0 indicates that a typical hard-sphere trajectory involves a sequence of backscattering collisions with its neighboring particles in the first coordination shell.

One of the most interesting features observed in Figs. 1 and 2 is that, while the decay rates of the VACFs and the FACFs are similar at a given ionic concentration, large differences exist between these correlation functions. In comparison with the VACF_+, the FACF_+ are observed to possess much deeper negative tails particularly for the systems at lower ρ_+ and η_0 values. In the simulation work of Heyes and Sandberg for dense Lennard–Jones systems [19], it was observed that the minimum in the FACF coincides approximately with the cross-over time at which the VACF first changes sign from positive to negative values. One would expect that, in dense systems, the cage effect induced by nearest neighbors dominate the motion of the central particle. This is not the case for dilute electrolyte systems where the electrostatic interaction between unlike pairs of ions tends to create ionic clusters or

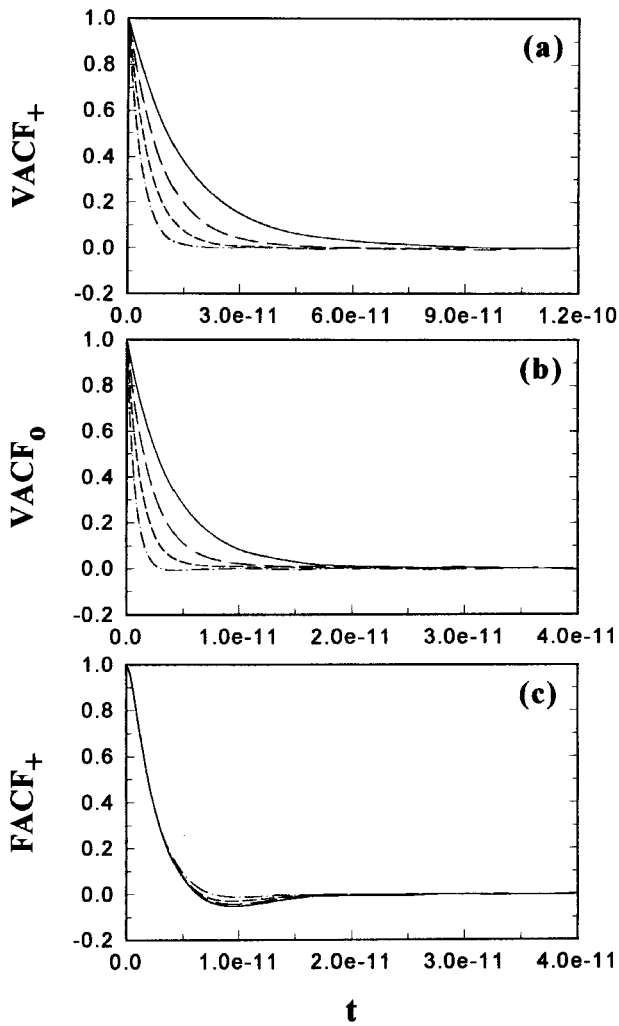

FIGURE 1 (a) Normalized VACFs vs. t for positively charged ions ($\rho_+ = 0.1$), (b) Normalized VACFs vs. t for neutral hard-spheres ($\rho_+ = 0.1$), and (c) Normalized FACFs vs. t for positively charged ions ($\rho_+ = 0.1$). The solid, the long-dashed, the short-dashed, and the chain-dotted curves correspond to $\eta_0 = 0.1$, $\eta_0 = 0.2$, $\eta_0 = 0.3$, and $\eta_0 = 0.4$, respectively.

aggregates. The individual ion particles change their momentum via chattering collisions with their neighbors, while a persistence of velocity is maintained in the original direction of cluster motion. Because the ionic clusters move coherently over a period of time longer than the mean time between ion collisions within the cluster, the VACF has a longer positive

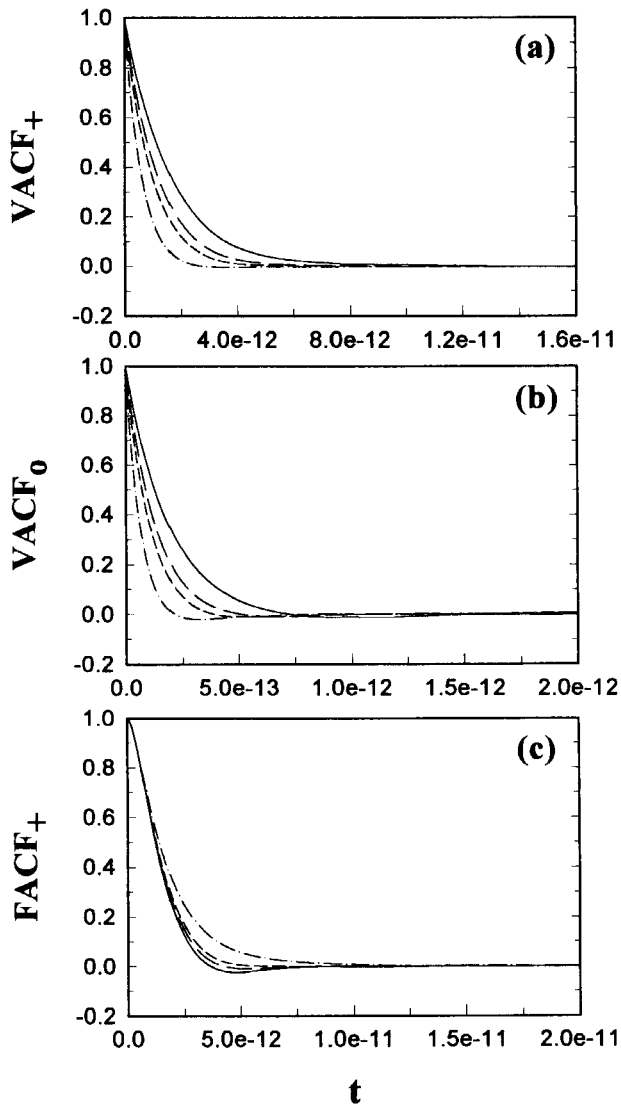

FIGURE 2 As in Fig. 1 but for $\rho_+ = 2.0$.

correlation than the FACF. The less negative correlation in the FACFs for higher η_0 values, which is opposite to the VACFs, can be explained by the fact that, at higher packing fractions of hard-spheres, the excluded volume effect enhances the formation of larger clusters and this causes restrictions in the coherent motion of ionic clusters.

This last point is clearly illustrated in Fig. 3 where the mean cluster size S is plotted as a function of cluster cutoff distance, R_{cl}. In our cluster algorithm a pair of dissimilarly charged ions is considered to be within the same cluster if the relative distance between the pair of ions is smaller than a given value of R_{cl}. A similar cluster definition was used in previous simulation studies of 2:2 electrolyte solutions using stochastic Langevin dynamics [20]. The mean cluster size S is obtained from the cluster size distribution using

$$S = \frac{\sum_s s^2 \bar{n}(s)}{\sum_s s \bar{n}(s)} \tag{9}$$

where s represents cluster size, and $\bar{n}(s)$ the mean number of clusters of size s. In this work we consider two types of clusters, namely, directly and indirectly bound clusters. Directly bound ions are simply those pairs, which satisfy the geometric cutoff criterion, while indirectly bound ions are connected through intermediate neighboring ions. Such a cluster analysis was implemented using the efficient approach for sampling cluster statistics proposed by Sevick *et al.* [21].

Figure 3 indicates that cluster formation is gradually enhanced with increasing hard-sphere packing fraction η_0. For example, the direct and the indirect mean cluster sizes S within $R_{cl} = 2.0\sigma_+$ are 1.47 and 1.66 at $\rho_+ = 0.1$ and $\eta_0 = 0.1$, and 1.64 and 2.04 at $\rho_+ = 0.1$ and $\eta_0 = 0.4$ as shown in Fig. 3a; the corresponding S values within $R_{cl} = 1.2\sigma_+$ are 1.95 and 3.38 at $\rho_+ = 2.0$ and $\eta_0 = 0.1$, and 2.50 and 12.34 at $\rho_+ = 2.0$ and $\eta_0 = 0.4$ as shown in Fig. 3b. A somewhat large difference between the results for directly and the indirectly bound clusters, particularly in the case of $\rho_+ = 2.0$, suggests the possibility of complex ion cluster formation.

For hard-sphere systems [22], the collision frequencies can be expressed in terms of the contact values of the radial distribution functions

$$\omega_{ij} = \pi\sigma_{ij}^2 \sqrt{\frac{8kT}{\pi\mu_{ij}}} \rho_j g_{ij}(\sigma_{ij}) \tag{10}$$

where ω_{ij} is the number of collisions per particle of component i per unit time between particles of component i and j, and $\mu_{ij}(= m_i m_j/(m_i + m_j))$ is the reduced mass. The total collision frequency for component i is simply

$$\omega_i = \sum_{j=1}^{m} \omega_{ij} \tag{11}$$

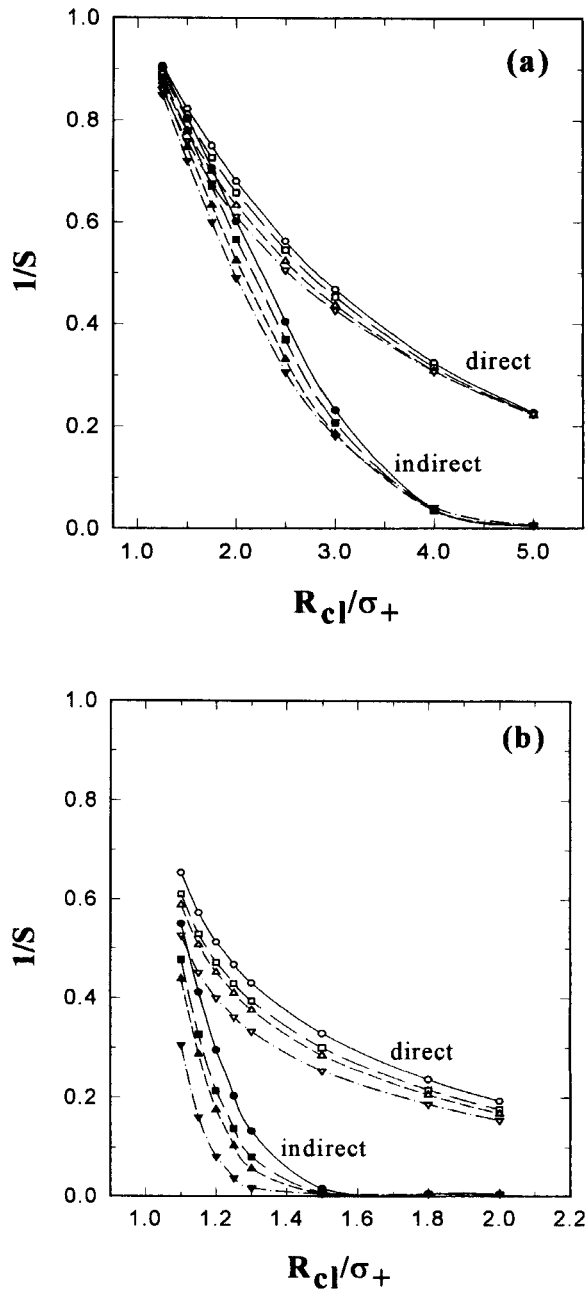

FIGURE 3 The inverse mean cluster size as a function of cluster distance, (a) $\rho_+ = 0.1$ and (b) $\rho_+ = 2.0$. The symbol of the circle, the square, the upward triangle, and the downward triangle correspond to $\eta_0 = 0.1$, $\eta_0 = 0.2$, $\eta_0 = 0.3$, and $\eta_0 = 0.4$, respectively.

In Fig. 4 the collision frequencies vs. η_0 determined from the MD simulation are illustrated for solute ions, ω_+ (Fig. 4a), and solvent hard-spheres, ω_0 (Fig. 4b), respectively. For the purpose of comparison with the corresponding hard-sphere systems, theoretical predictions for the collision frequencies obtained using Eq. (10) in conjunction with contact values for the radial distribution functions computed directly from the MD simulations are also shown as the dotted curves in these figures. The MD results are seen to be in excellent agreement with hard-sphere approximations over a wide range of η_0 and σ_0. This suggests that the microscopic dynamics of the SPM electrolyte solutions investigated in this work are very similar to the dynamical processes taking place in neutral hard-sphere mixtures. In this sense the transport properties of 1:1 SPM systems are, at least qualitatively, related to those for hard-sphere fluids.

In previous MD simulations of 1:1 PM electrolyte solutions [13], the Enskog theory of hard-spheres was shown to predict the self-diffusion coefficients reasonably accurately. Such a modified Enskog approximation for PM electrolytes can also be extended to the SPM electrolyte systems. In the extended Enskog theory the self-diffusion coefficient for component i can be expressed in terms of the intradiffusion coefficients for multicomponent mixtures,

$$D_{E,i} = \left(\sum_{j=1}^{m} \frac{\rho_j g_{ij}(\sigma_{ij})}{(\rho D_{ij})_0} \right)^{-1} \tag{12}$$

and

$$(\rho D_{ij})_0 = \frac{3}{8\sigma_{ij}^2} \sqrt{\frac{kT}{2\pi\mu_{ij}}} \tag{13}$$

where $(\rho D_{ij})_0$ represents the product of the number density and the binary mutual diffusion coefficient in the dilute gas limit of hard-spheres.

In Fig. 5 the self-diffusion coefficients obtained from the MD simulations are compared with those predicted using the extended Enskog theory in Eqs. (12) and (13). The MD data for the diffusivities were calculated from the integration of the corresponding VACF using the Green–Kubo relationship. Again, it is observed that the theoretical predictions and the MD calculations are in good agreement. One should recall however that, while the Enskog theory takes advantage of the simplification that the properties of a dense fluid are primarily determined by the repulsive core of the particle–particle interaction, it does have limitations, particularly a high density. The error involved in using the Enskog theory under these conditions are ascribed to the failure of the molecular-chaos approximation and the deviations are most pronounced when the cage effect is important. For

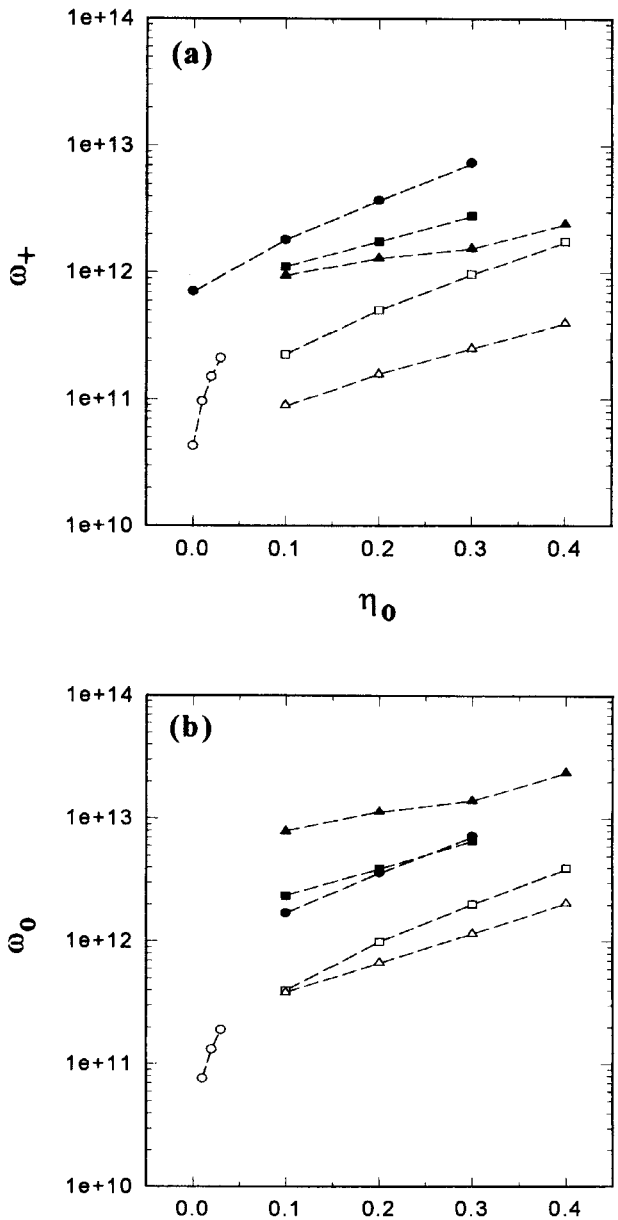

FIGURE 4 Semilogarithmic plot for collision frequency as a function of η_0. (a) positively charged ions and (b) neutral hard-spheres. The symbol of the circle, the square, and the triangle correspond to $\sigma_0 = \sigma_+$, $\sigma_0 = 2\sigma_+$, and $\sigma_0 = 5\sigma_+$, and the open and filled symbols represents $\rho_+ = 0.1$ and $\rho_+ = 2.0$, respectively. The dotted curves are theoretical predictions provided by Eqs. (10) and (11) using the MD contact values for the radial distribution functions.

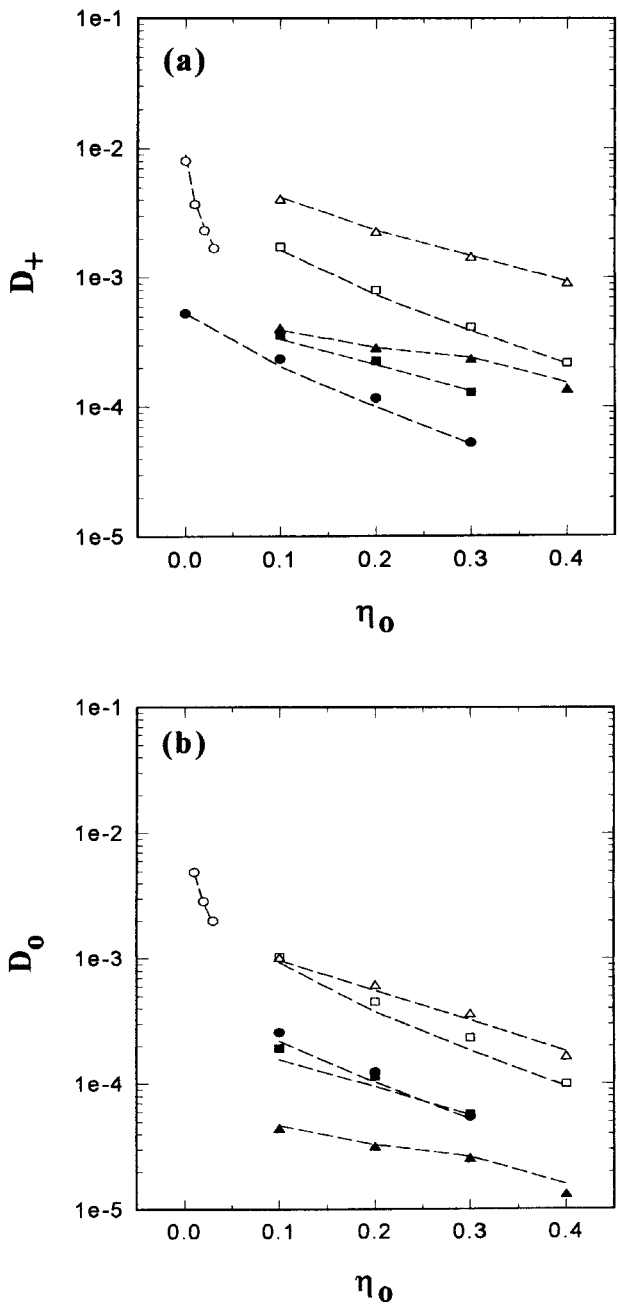

FIGURE 5 Semilogarithmic plot for self-diffusion coefficient as a function of η_0. (a) positively charged ions and (b) neutral hard-spheres. The symbols are the same as in Fig. 4. The dotted curves are theoretical predictions provided by Eqs. (12) and (13) in conjunction with the MD contact values for the radial distribution functions.

mixtures of 1:3 PM electrolytes [14], it was found that the self-diffusion coefficients of the lower charged electrolytes were close to those for 1:1 PM electrolytes, whereas those of highly charged electrolytes were smaller by a factor of two or three. An interpretation of this observation is that the free motion of highly charged ions is likely to be restricted by the formation of ionic clusters.

CONCLUSION

In the present work MD simulations at constant temperature have been carried out to investigate the equilibrium thermodynamic and time-dependent transport properties of 1:1 solvent PM electrolyte solutions. MD results for the excess internal energy and the osmotic pressure are shown to be in good agreement with the mean spherical approximation, and, more precisely, with the hypernetted chain theory. In the lower concentration regime, the electrostatic interaction plays an important role in determining ion trajectories, while the hard-sphere collisions dominate in the higher concentration regime.

Significant differences are also observed between the VACFs and FACFs. The less negative correlation effects displayed by the FACFs at higher hard-sphere packing fractions are related to a restricted coherent motion of the larger ionic clusters, which are formed at these densities. This conclusion is supported by an independent analysis of the direct and indirect bound ion cluster size distributions computed during the MD simulations. Under the conditions employed in this work, excellent agreement is also observed between the MD results and the theoretical predictions for the self-diffusion coefficients and the collision frequencies of both ionic solute and hard-sphere solvent. In this respect our simulation studies strongly suggest that by incorporating the discrete particulate nature of the solvent into models of electrolyte solutions, then the interpretation of the nonequilibrium as well as equilibrium phenomena taking place within such systems should be significantly improved.

Acknowledgements

This work was supported by a grant from KOSEF and the assistance of computing resources from KISTI. JWP is also grateful to his graduate stipend through the BK21 project.

References

[1] Durand-Vidal, S., Simonin, J.-P. and Turq, P. (2000) Electrolytes at Interfaces (Kluwer Academic Publishers, Dordrecht).

[2] Tang, Z., Scriven, L.E. and Davis, H.T. (1992) "A three-component model of the electrical double layer", *J. Chem. Phys.* **97**, 494–503.

[3] Zhang, L., Davis, H.T. and White, H.S. (1993) "Simulations of solvent effects on confined electrolytes", *J. Chem. Phys.* **98**, 5793–5799.

[4] Tang, Z., Scriven, L.E. and Davis, H.T. (1994) "Effects of solvent exclusion on the force between charged surfaces in electrolyte solution", *J. Chem. Phys.* **100**, 4527–4530.

[5] Forciniti, D. and Hall, C.K. (1994) "Structural properties of mixtures of highly asymmetrical electrolytes and uncharged particles using the hypernetted chain approximation", *J. Chem. Phys.* **100**, 7553–7566.

[6] Rescic, J., Vlachy, V., Bhuiyan, L.B. and Outhwaite, C.W. (1997) "Monte Carlo simulation studies of electrolyte in mixture with a neutral component", *J. Chem. Phys.* **107**, 3611–3618.

[7] Rescic, J., Vlachy, V., Bhuiyan, L.B. and Outhwaite, C.W. (1998) "Monte Carlo simulations of a mixture of an asymmetric electrolyte and a neutral species", *Mol. Phys.* **95**, 233–242.

[8] Wu, G.-W., Lee, M. and Chan, K.-Y. (1999) "Grand canonical Monte Carlo simulation of an electrolyte with a solvent primitive model", *Chem. Phys. Lett.* **307**, 419–424.

[9] Hribar, B. and Vlachy, V. (1997) "Evidence of electrostatic attraction between equally charged macroions induced by divalent counterions", *J. Phys. Chem. B* **101**, 3457–3459.

[10] Hribar, B. and Vlachy, V. (2000) "Clustering of macroions in solutions of highly asymmetric electrolytes", *Biophys. J.* **78**, 694–698.

[11] Allen, M.P. and Tildesley, D.J. (1987) Computer Simulation of Liquids (Oxford Science Publications.

[12] McNeil, W.J. and Madden, W.G. (1982) "A new method for the molecular dynamics simulation of hard core molecules", *J. Chem. Phys.* **76**, 6221–6226.

[13] Heyes, D.M. (1982) "Molecular dynamics simulations of restricted primitive model 1:1 electrolytes", *Chem. Phys.* **69**, 155–163.

[14] Suh, S.-H., Mier-y-Teran, L., White, H.S. and Davis, H.T. (1990) "Molecular dynamics study of the primitive model of 1-3 electrolyte solutions", *Chem. Phys.* **142**, 203–211.

[15] Houndonougbo, Y.A., Laird, B.B. and Leimkuhler, B.J. (2000) "A molecular dynamics algorithm for mixed hard-core/continuous potentials", *Mol. Phys.* **98**, 309–316.

[16] Brush, S.G., Sahlin, H.L. and Teller, E. (1966) "Monte Carlo study of a one-component plasma. I", *J. Chem. Phys.* **45**, 2102–2118.

[17] Berendsen, H.J.C., Postma, J.P.M., van Gunsteren, W.F., DiNola, A. and Haak, J.R. (1984) "Molecular dynamics with coupling to an external bath", *J. Chem. Phys.* **81**, 3684–3690.

[18] Sanchez-Castro, C. and Blum, L. (1989) "Explicit approximation for the unrestricted mean spherical approximation for ionic solutions", *J. Chem. Phys.* **93**, 7478–7482.

[19] Heyes, D.M. and Sandberg, W.C. (1990) "Microscopic motion of atoms in simple liquids at equilibrium and with shear flow", *Phys. Chem. Liq.* **22**, 31–50.

[20] Abascal, J.L.F., Bresme, F. and Turq, P. (1994) "The influence of concentration and ionic strength on the cluster structure of highly charged electrolyte solutions", *Mol. Phys.* **81**, 143–156.

[21] Sevick, E.M., Monson, P.A. and Ottino, J.M. (1987) "Monte Carlo calculations of cluster statistics in continuum models of composite morphology", *J. Chem. Phys.* **88**, 1198–1206.

[22] McQuarrie, D.A. (1976) Statistical Mechanics (Harper and Row, New York).